ELSEVIER

Physica B 221 (1996) 34–43

PHYSICA B

Effect of roughness correlations in multilayers on Bragg peaks in X-ray diffuse scattering

V.M. Kaganer [a, b], S.A. Stepanov [a, c, *], R. Köhler [a]

[a] *MPG-AG "Röntgenbeugung", Hausvogteiplatz 5–7, Berlin D-10117, Germany*
[b] *Institute of Crystallography, Russian Academy of Sciences, Leninskii pr.59, Moscow 117333, Russian Federation*
[c] *Institute of Nuclear Problems, 11 Bobruiskaya St., Minsk 220050, Belarus*

Abstract

The peaks in X-ray diffuse scattering associated with the diffraction of the incident or scattered waves from a periodically layered structure are investigated analytically and compared with numerical calculations. It is shown that if the roughness of the periodic interfaces is uncorrelated, the peaks follow the intensity of the X-ray standing wave at the interfaces. Interference effects due to correlated interfacial roughness can change the sense of the peak (sequence of maximum and minimum). The factors controlling the peak sense are derived and applied to explain the results of numerical calculations.

1. Introduction

X-ray diffuse scattering has proven to be an informative and non-destructive tool applicable to studies of roughness of surfaces and interfaces in at least five fields of application: semiconductor multilayers for advanced electronic devices [1–5], multilayers fabricated for use as optical elements for soft X-rays [6–12], epitaxial film growth [13–15], thermal fluctuations of liquid surfaces and fluid films [16–19], organic multilayers on solid substrates (Langmuir–Blodgett films) [20] (see also the review Ref. [21]).

An essential feature of diffuse scattering from multilayer systems is the sensitivity to correlations between the roughnesses of interfaces. This effect is especially pronounced in periodic multilayers. When the roughness of periodic interfaces is correlated, diffuse intensity is concentrated on equidistantly spaced sheets in the reciprocal space. This effect has been observed and then explained almost simultaneously on different multilayer systems (to the best of our knowledge, the effect was first pointed out in theoretical studies by Andreev et al. [22] but remained unclaimed and rediscovered in the experimental studies cited above). All experimental studies report that the roughness of different interfaces is correlated, at least partially.

Additional singularities in the diffuse scattering spectra are observed when either the incident or scattered beam occurs in Bragg diffraction conditions due to the periodicity of multilayer. The shape of these singularities can be especially sensitive to an asymmetry between B/A and A/B interfaces in periodic multilayers [23]. It has been claimed, without proof, that the intensity distribution in Bragg singularities follows the standing wave intensity at interfaces [8, 24]. The aim of this paper is to investigate the formation of these singularities and their sensitivity to interlayer roughness correlations by means of analytical estimations compared with numerical calculations. We show that the Bragg-diffraction peaks in diffuse scattering follow exactly the standing wave distribution only if the roughness of different interfaces is purely uncorrelated. We demonstrate that in presence of correlations the sense of the peaks (i.e., the sequence of maxima and minima) can be opposite, and derive a factor controlling it.

2. The reciprocity theorem

The most effective way to calculate the intensity of X-ray diffuse scattering is to apply the reciprocity theorem. Its

* Corresponding author.

0921-4526/96/$15.00 © 1996 Elsevier Science B.V. All rights reserved
SSDI 0921-4526(95)00902-7

formulation employed by Sinha et al. [25] and frequently referred to is based on the quantum mechanical theorem and uses the terminology of "time-reversed states" which in practical application can be confusing for X-ray scattering problems. A more direct way is to use the reciprocity theorem of electrodynamics. For the first time it was applied to the problems of X-ray diffraction by Laue [26] for analysis of distribution of X-rays scattered by atoms in crystals (Kossel lines). In the derivation below we follow the paper [27] by one of us.

Consider plane wave $\boldsymbol{e}_0 \exp(\mathrm{i}\boldsymbol{k}_0\boldsymbol{r})$ illuminating a scattering object (crystal, multilayer, etc.). Its scattering from an "ideal" object containing no fluctuations and possessing the polarizability $\chi_{\mathrm{id}}(\boldsymbol{r})$ gives rise to the coherent wave field $\boldsymbol{E}^{\mathrm{in}}(\boldsymbol{r})$ inside the object whose explicit form can be found as a solution to the corresponding problem of X-ray optics, taking into account refraction, diffraction, and reflection phenomena. The fluctuations of polarizability cause a perturbation $\delta\chi(\boldsymbol{r}) = \chi(\boldsymbol{r}) - \chi_{\mathrm{id}}(\boldsymbol{r})$ and give rise to the additional current $\boldsymbol{j}_1 = -(\mathrm{i}\omega/4\pi)\delta\chi\boldsymbol{E}^{\mathrm{in}}$ entering Maxwell equations. The radiation field of this current far from the scattering object is $\boldsymbol{E}_1 = (f/r)\boldsymbol{e}_1 \exp(\mathrm{i}kr)$, where $f \equiv f(\boldsymbol{e}_1, \boldsymbol{k}_1, \boldsymbol{e}_0, \boldsymbol{k}_0)$ is the scattering amplitude to be found. It describes the scattering of the incident wave with the wave vector $\boldsymbol{k}_0$ and polarization $\boldsymbol{e}_0$ into the wave with the wave vector $\boldsymbol{k}_1$ and polarization $\boldsymbol{e}_1$, and $k = |\boldsymbol{k}_0| = |\boldsymbol{k}_1|$.

To determine the scattering amplitude, let us make use of the reciprocity theorem of electrodynamics [28] which relates the electric fields $\boldsymbol{E}$ and $\boldsymbol{E}'$ due to the two arbitrary currents $\boldsymbol{j}$ and $\boldsymbol{j}'$ by the equality $\int \boldsymbol{E}\boldsymbol{j}'\,\mathrm{d}V = \int \boldsymbol{E}'\boldsymbol{j}\,\mathrm{d}V$. In addition to the field $\boldsymbol{E}_1$ of the current $\boldsymbol{j}_1$, we introduce the field $\boldsymbol{E}^{\mathrm{out}}$ of the current $\boldsymbol{j}^{\mathrm{out}}$, which can be chosen arbitrarily. The reciprocity theorem gives

$$\int \boldsymbol{E}^{\mathrm{out}}\boldsymbol{j}_1\,\mathrm{d}V = \int \boldsymbol{E}_1\boldsymbol{j}^{\mathrm{out}}\,\mathrm{d}V. \tag{1}$$

Integration in Eq. (1) is performed over the regions where the currents $\boldsymbol{j}_1$ and $\boldsymbol{j}^{\mathrm{out}}$ are non-zero. Let us choose the current $\boldsymbol{j}^{\mathrm{out}}$ as $\boldsymbol{j}^{\mathrm{out}}(\boldsymbol{r}) = -(\mathrm{i}\omega/k^2)R\,\boldsymbol{e}_1^* \exp(\mathrm{i}kr)\delta(\boldsymbol{r} - \boldsymbol{R})$ in the observation point $\boldsymbol{R}$ disposed far from the scattered object. This current produces a plane wave $\boldsymbol{e}_1^* \exp(-\mathrm{i}\boldsymbol{k}_1\boldsymbol{r})$ illuminating the object. The field $\boldsymbol{E}^{\mathrm{out}}$ in the object due to this current is the solution to the problem of X-ray optics for the "reversed" scattered wave $\boldsymbol{e}_1^* \exp(-\mathrm{i}\boldsymbol{k}_1\boldsymbol{r})$. Then Eq. (1) gives the scattering amplitude

$$f = (k^2/4\pi)\int \boldsymbol{E}^{\mathrm{out}}(\boldsymbol{r})\delta\chi(\boldsymbol{r})\boldsymbol{E}^{\mathrm{in}}(\boldsymbol{r})\,\mathrm{d}V. \tag{2}$$

The reciprocity theorem has allowed us to reduce the problem of determining the radiation field of the current disposed inside the scattering object to the well-known problem of X-ray optics of ideal (non-fluctuating) system. Eq. (2) does not involve any complex conjugation or "time inversion", and both wave fields, $\boldsymbol{E}^{\mathrm{in}}$ and $\boldsymbol{E}^{\mathrm{out}}$, are absorbed when propagating into the object. Eq. (2) is applicable in case of arbitrary anisotropic absorbing non-uniform media. If the perturbation of polarizability $\delta\chi(\boldsymbol{r})$ is time-dependent, the wave fields $\boldsymbol{E}^{\mathrm{in}}$ and $\boldsymbol{E}^{\mathrm{out}}$ possess different frequencies, thus describing inelastic scattering (the undisturbed polarizability $\chi_{\mathrm{id}}(\boldsymbol{r})$ is considered to be time-independent in order to ensure the applicability of the reciprocity theorem). Approximation (2) is commonly referred to as the distorted wave born approximation (DWBA). Far from the regions of diffraction or reflection the waves $\boldsymbol{E}^{\mathrm{in}}$ and $\boldsymbol{E}^{\mathrm{out}}$ tend to plane waves, $\boldsymbol{E}^{\mathrm{in}} = \boldsymbol{e}_0 \exp(\mathrm{i}\boldsymbol{K}^{\mathrm{in}}\boldsymbol{r})$ and $\boldsymbol{E}^{\mathrm{out}} = \boldsymbol{e}_1^* \exp(\mathrm{i}\boldsymbol{K}^{\mathrm{out}}\boldsymbol{r})$, where $\boldsymbol{K}^{\mathrm{in}}$ and $\boldsymbol{K}^{\mathrm{out}}$ are the wave vectors inside the medium that differ from corresponding vacuum waves $\boldsymbol{k}_0$ and $-\boldsymbol{k}_1$ due to refraction. The scattering amplitude (2) reduces to

$$f = (k^2/4\pi)\delta\chi(\boldsymbol{Q}), \quad \boldsymbol{Q} = -(\boldsymbol{K}^{\mathrm{in}} + \boldsymbol{K}^{\mathrm{out}}), \tag{3}$$

with $\delta\chi(\boldsymbol{Q})$ being the Fourier transform of $\delta\chi(\boldsymbol{r})$. When the refraction can be neglected, the wave-vector transfer $\boldsymbol{Q}$ inside the medium is reduced to the vacuum wave-vector transfer $\boldsymbol{q} = \boldsymbol{k}_1 - \boldsymbol{k}_0$. Thus, Eq. (3) is the refraction-corrected first Born approximation. Hereafter, we do not consider polarization phenomena and write Eq. (3) for an eigen polarization (σ or π). We stress that, by definition of the wave fields $\boldsymbol{E}^{\mathrm{in}}$ and $\boldsymbol{E}^{\mathrm{out}}$, both wave vectors $\boldsymbol{K}^{\mathrm{in}}$ and $\boldsymbol{K}^{\mathrm{out}}$ are directed inside the medium and $\boldsymbol{K}^{\mathrm{out}} \approx -\boldsymbol{k}_1$, when refraction is neglected. The mean value $\langle\delta\chi(\boldsymbol{Q})\rangle$ of the fluctuating part of polarizability contributes to the coherent scattering and the deviation

$$\delta\chi'(\boldsymbol{Q}) = \delta\chi(\boldsymbol{Q}) - \langle\delta\chi(\boldsymbol{Q})\rangle \tag{4}$$

gives rise to diffuse scattering.

3. Diffuse scattering on periodic rough interfaces

The periodicity of the scattering object gives rise to singularities in diffuse scattering distribution. In this section we consider the features of the diffuse scattering according to the Born approximation (3). It is applicable if the incidence and exit angles are large compared with the critical angle for total external reflection and do not coincide with any Bragg angle due to periodic structure. In fact, these restrictions leave the Born approximation applicable to the major part of diffuse scattering distribution. The Born approximation for the differential cross section of diffuse scattering due to rough interfaces between layers is

$$\mathrm{d}\sigma/\mathrm{d}\Omega = (k^2/4\pi)^2 \sum_{j,k} \langle\delta\chi_j'(\boldsymbol{Q})\delta\chi_k'^*(\boldsymbol{Q})\rangle, \tag{5}$$

where summation is performed over the interfaces. When calculating the Fourier transform of the polarizability fluctuations $\delta\chi_j'(\boldsymbol{Q})$ on jth interface, it is convenient to shift the

origin to the mean interface position z_j, which gives rise to the phase term $\exp(-iQ_z z_j)$. Then, the correlations of polarizability fluctuations on different interfaces can be represented as

$$\langle \delta\chi_j'(\boldsymbol{Q}_1)\delta\chi_k'^*(\boldsymbol{Q}_2)\rangle = \Delta\chi_j\Delta\chi_k \exp[-i(Q_{1z}z_j - Q_{2z}^* z_k)] \times C_{jk}(Q_{1z}, Q_{2z}, \boldsymbol{q}_\perp). \quad (6)$$

Here $\Delta\chi_j$ is the polarizability jump at jth interface and $C_{jk}(Q_{1z}, Q_{2z}, \boldsymbol{q}_\perp)$ is a correlation function, the explicit form of which depends on the model of roughness. We discuss it in Section 5. Although in the Born approximation (5) the correlations of polarizability fluctuations are required for $Q_{1z} = Q_{2z} = Q_z$ only, a more general formula (6) will be helpful in further analysis. The component $\boldsymbol{q}_\perp$ in the plane of the layers is the same for all wave vectors of the problem, due to the translational invariance in that plane. C_{jk} is a smooth function of its variables. In the simplest case of roughness caused by small random displacements $u_j(\boldsymbol{\rho})$ of interfaces, so that $Q_z^2\langle u_j^2\rangle \ll 1$, it is reduced to the two-dimensional Fourier transform of the function $C_{jk}(\boldsymbol{\rho}) = \langle u_j(\boldsymbol{\rho})u_k(0)\rangle$ and does not depend on Q_{1z} and Q_{2z}, see Section 5.

Two limiting cases of interface–interface roughness correlations are uncorrelated roughness, $C_{jk} = C_j\delta_{jk}$, and completely correlated roughness, $C_{jk} = C$. Consider a slab of N periods of thickness $D = d_1 + d_2$, each period consisting of two layers with thicknesses d_1 and d_2 and polarizabilities χ_1 and χ_2, respectively. One has to take into account that the polarizability jump at jth interface $\Delta\chi_j$ has an opposite sign on neighboring interfaces: $\Delta\chi_j = (-1)^j\Delta\chi$, where $\Delta\chi = \chi_2 - \chi_1$. For uncorrelated roughness, one readily obtains

$$d\sigma/d\Omega = (k^2\Delta\chi/4\pi)^2 \sum_j C_j(Q_z, Q_z, \boldsymbol{q}_\perp). \quad (7)$$

Eq. (7) describes a smooth distribution of intensity. For completely correlated roughness the substitution of Eq. (6) into Eq. (5) gives

$$\frac{d\sigma}{d\Omega} = \left(\frac{k^2\Delta\chi}{2\pi}\right)^2 C(Q_z, Q_z, \boldsymbol{q}_\perp)\sin^2\frac{Q_z d_1}{2}\Phi^2(Q_z), \quad (8)$$

where

$$\Phi(Q_z) = \frac{\sin(Q_z ND/2)}{\sin(Q_z D/2)}. \quad (9)$$

The number of layers is supposed to be large enough, so that the contributions of surface and the interface between the substrate and multilayer can be taken equal to that of interfaces in multilayer. The behavior of function $\Phi^2(Q_z)$ is well known: it possesses equidistantly spaced maxima at $Q_z = 2\pi m/D$ (where m is an integer), the height of which is N^2 and the width is proportional to N^{-1}. Thus, the intensity of the diffuse scattering concentrates on the sheets $Q_z = 2\pi m/D$, as a result of interference between waves diffusely scattered at different interfaces. This effect of resonant diffuse scattering (RDS) has been observed and explained for several multilayer systems [1, 2, 4, 6–10, 12, 21].

4. Bragg-diffraction peaks in diffuse scattering

4.1. Cross-section of diffuse scattering

When either incident or scattered waves occur in Bragg-diffraction conditions, the corresponding wave is no longer a plane wave and the Born approximation (3) is not valid. The diffracted wave has to be taken into account. The diffraction process close to a diffraction vector $H = 2\pi m/D$ can be considered as a scattering from the corresponding Fourier component of polarizability of the periodic system

$$\chi_H = \frac{4}{HD}\Delta\chi\exp(-iHd_1/2)\sin(Hd_1/2). \quad (10)$$

The phase factor $\exp(-iHd_1/2)$ arises due to the distance $z = d_1/2$ of the symmetry plane of multilayer "unit cell" from the origin $z = 0$ chosen at the multilayer surface. Dynamical diffraction effects are governed by the ratio of the extinction length $\Lambda_H = 2\sin\theta/(k|\chi_H|)$ for the corresponding Bragg reflection to the thickness $L = ND$ of multilayer. The extinction length increases systematically with the reflection order due to an increase in the incidence angle θ as well as a decrease in χ_H. As a result, in most practical cases, it is larger than the multilayer thickness for $m > 1$. This conclusion follows also from the experimental curves of specular reflectivity, see e.g. Ref. [4, 6, 7, 10, 21]: the reflectivity at Bragg maxima occurs much smaller than unity with the exception of the first Bragg peak. Then the kinematical approximation can be applied to determine the wave fields E^{in} and E^{out}. Under kinematical diffraction conditions, the diffraction peak intensity is proportional to $|\chi_H|^2 \sim m^{-2}\sin^2(\pi m d_1/D)$, giving rise to a systematic intensity decrease with the diffraction order as m^{-2} and additional dumping of some peaks when md_1/D is close to an integer value. We note that the same term $\sin^2(Qd_1/2)$ governs the intensity of the RDS sheets in Eq. (8). Thus, the RDS peaks in diffuse scattering are dumped simultaneously with the corresponding specular reflectivity peaks.

The Bragg-diffraction condition for a given reciprocal lattice vector $\boldsymbol{H}$ is satisfied for the incident wave along a line in the scattering plane (q_x, q_z). This line intersects the lines where the Bragg-diffraction condition is satisfied for scattered wave with reciprocal vectors $\boldsymbol{H}'$. Generally speaking, the diffraction of both incident and scattered waves should be taken into account at the intersections. However, the systematic decrease in kinematic diffraction proportional to H^{-2} gives rise to considerably different contributions from two processes for $H \neq H'$ (the lines with $H = H'$ intersect at

the position of specularly reflected beam). For this reason, we restrict ourselves to the diffraction of either incident or scattered waves. Simultaneous diffraction of both waves can be essential in case of dumping of one of the waves mentioned above and leads to overlapping of two singularities.

Let us for the sake of definiteness assume that Bragg diffraction conditions are satisfied for the incident wave. The solution of the two-wave dynamical diffraction problem (involving only one diffraction vector $\boldsymbol{H}$) for the ideal periodic structure is well known [29]. Its kinematical limit at $L \ll \Lambda_H$ is

$$E^{\text{in}}(\boldsymbol{r}) = \exp(\mathrm{i}\boldsymbol{K}^{\text{in}}\boldsymbol{r}) + \frac{\chi_H}{|\chi_H|}\exp[\mathrm{i}(\boldsymbol{K}^{\text{in}} + \boldsymbol{H})\boldsymbol{r}] \times \frac{1}{2\Lambda_H\kappa}\{1 - \exp[2\mathrm{i}\kappa(L - z)]\}. \quad (11)$$

Here $\boldsymbol{\kappa} = (\boldsymbol{K}^{\text{in}} - \boldsymbol{K}_B^{\text{in}})_z$ is the projection of the wave-vector deviation from the Bragg condition on z-axis directed normally to the interfaces.

Approximation (11) does not restrict possible values of κ, so that the phase factor in the last term generally is not small. In the limit $\kappa \to 0$, the wave field in the origin $\boldsymbol{r} = 0$, chosen at the entrance surface of the structure, is $E^{\text{in}}(0) = 1 - \mathrm{i}k\chi_H L/(2\sin\theta)$. It is proportional to χ_H and the slab thickness L. This limiting case can be derived in the simplest approximation of quantum mechanical perturbation theory. To derive general expression (11), one can employ the perturbation theory applicable in the case of large energies [30]. In the limit $\kappa \gg \Lambda_H^{-1}$, the second term decreases as κ^{-1}, as it should be in the kinematical approximation. The second term on the right-hand side of Eq. (11) remains small in comparison with the first one due to the restriction $L \ll \Lambda_H$.

The two terms in wavy brackets can be treated as if they are due to a direct diffraction at point $\boldsymbol{r}$ and reflection from the bottom surface of the slab, respectively. Substituting Eq. (11) into Eq. (2) and taking the reversed scattered wave as a plane wave $E^{\text{out}} = \exp(\mathrm{i}\boldsymbol{K}^{\text{out}}\boldsymbol{r})$, one has

$$\frac{\mathrm{d}\sigma}{\mathrm{d}\Omega} = \left(\frac{k^2}{4\pi}\right)^2 \Big\{\langle\delta\chi'(\boldsymbol{Q})\delta\chi'^*(\boldsymbol{Q})\rangle + \frac{1}{\Lambda_H\kappa}\mathrm{Re}\frac{\chi_H}{|\chi_H|} \times [\langle\delta\chi'(\boldsymbol{Q} - \boldsymbol{H})\delta\chi'^*(\boldsymbol{Q})\rangle - \exp(2\mathrm{i}\kappa L)\langle\delta\chi'(\boldsymbol{Q} - \boldsymbol{H} + 2\boldsymbol{\kappa})\delta\chi'^*(\boldsymbol{Q})\rangle]\Big\}. \quad (12)$$

The first term in Eq. (12) was obtained in the Born approximation (3) and the two other terms are due to the direct diffraction of the incident wave and the wave scattered from the bottom surface of the slab, respectively. By comparing them with the result of the Born approximation, one can see that they involve correlations between fluctuations of polarizability on two different wave vectors and thus, in principle, contain more detailed information about correlations.

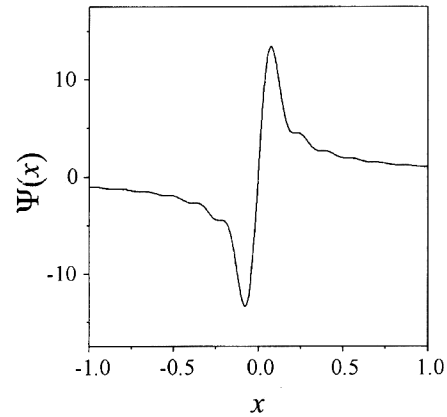

Fig. 1. Function $\Psi(x)$ (Eq. (15)) controlling standing-wave-like effects in X-ray diffuse scattering from periodic multilayers. $N = 20$.

4.2. Uncorrelated roughness

Consider first uncorrelated roughness of the interfaces and put $C_{jk} = C\delta_{jk}$. Then, keeping in mind that κ is small in comparison with Q_z and H, and $\kappa d_1 \ll 1$, one arrives at

$$\frac{\mathrm{d}\sigma}{\mathrm{d}\Omega} = 2N\left(\frac{k^2\Delta\chi}{4\pi}\right)^2 C(Q_z, Q_z, \boldsymbol{q}_\perp)[1 + g\xi S_{\text{u}}\Psi(\kappa D)]. \quad (13)$$

Here $g = 4k^2\Delta\chi/H^2$, and $\xi = C(Q_z, Q_z - H, \boldsymbol{q}_\perp)/C(Q_z, Q_z, \boldsymbol{q}_\perp)$ is a factor of the order of unity, and

$$S_{\text{u}} = \sin(Hd_1) \quad (14)$$

is a factor determining the sign and magnitude of the Bragg-diffraction effect. The function

$$\Psi(x) = x^{-1}[1 - \cos((N+1)x)\sin(Nx)/(N\sin x)] \quad (15)$$

of the argument $x = \kappa D$ is presented in Fig. 1. Let us calculate, for comparison, the total intensity of the wave field $E^{\text{in}}(\boldsymbol{r})$ on interfaces $\boldsymbol{r}_j = (\boldsymbol{\rho}, z_j)$:

$$I = \sum_j |E^{\text{in}}(\boldsymbol{\rho}, z_j)|^2 = 2N[1 + gS_{\text{u}}\Psi(\kappa D)]. \quad (16)$$

By comparing Eqs. (13) and (16), one can conclude that the diffuse scattering from multilayers with uncorrelated roughness follows the intensity of the X-ray standing wave (16) at the interfaces, differing from it only by slowly varying factor $\xi \sim 1$. The dispersion-like curve of Fig. 1 is typical for a standing wave. We note that Eq. (16) is derived on the basis of the kinematical approximation and Fig. 1 presents a small additional contribution to the intensity of the transmitted wave.

4.3. Correlated roughness

Let us proceed now to the opposite limiting case of completely correlated roughness and put $C_{jk} = C$ in Eq. (12). Then we obtain

$$\frac{d\sigma}{d\Omega} = \left(\frac{k^2\Delta\chi}{2\pi}\right)^2 \Phi^2(Q_z)C(Q_z, Q_z, \boldsymbol{q}_\perp) \times\{\sin^2(Q_z d_1/2) + g\xi S_c \Psi_c(\kappa D)\}, \quad (17)$$

where

$$\Psi_c(x) = (x)^{-1}[1 - \cos((N+1)x)\,\Phi(Q_z - 2\kappa)/\Phi(Q_z)] \quad (18)$$

and

$$S_c = \sin(Hd_1/2)\sin[(Q_z - H)d_1/2]\sin(Q_z d_1/2). \quad (19)$$

For the scan along a RDS maximum, Q_z is equal to one of the Bragg diffraction vectors $Q_z = G = 2\pi n/D$, and the function $\Psi_c(\kappa D)$ is reduced to $\Psi(\kappa D)$. Then the second term of Eq. (17) differs from that of Eq. (13) only by substitution of S_c for S_u.

Two terms S_c and S_u can differ in sign and magnitude, depending on the reciprocal-lattice vectors G and H. Thus, the peaks due to uncorrelated and correlated interface roughness can differ by magnitude and sense (sequence of maxima and minima). We present some numerical examples in the next section.

When $\kappa = 0$, i.e., for the scan over the exit angle while keeping the incident wave at the Bragg position, one has $\Psi_c = \Phi^{-2}d(\Phi^2)/dQ_z$ and Eq. (17) reduces to $\Phi^2(Q_z + \delta Q_z)$ where $\delta Q_z \sim gS_c$. Thus, the RDS peaks slightly shift when the incident (or scattered) wave satisfies the Bragg condition.

4.4. Sensitivity to correlations

Let us now consider the transition between two limiting cases of completely correlated and completely uncorrelated roughness. It can be analytically shown that the qualitative features of Bragg peaks are not sensitive to minor deviations from completely correlated roughness. To demonstrate this, let us take $Q_z = G$ and assume smooth variations of C_{jk} with j and k, so that for two interfaces belonging to one and the same period of the multilayer $C_{jk} \approx C_{j+1,k}$. One can then proceed to a summation over the periods with the correlation function C_{mn} and arrive at

$$\frac{d\sigma}{d\Omega} = \left(\frac{k^2\Delta\chi}{2\pi}\right)^2 \left\{\sin^2\frac{Gd_1}{2}\sum_{m,n=0}^{N-1} C_{mn}(G, G, \boldsymbol{q}_\perp) + gS_c(\kappa D)^{-1}\sum_{m,n=0}^{N-1} C_{mn}(G, G-H, \boldsymbol{q}_\perp)\sin^2\kappa(L - z_m)\right\}. \quad (20)$$

The Bragg-diffraction peak is due to the second term of Eq. (20). It involves a sum of positive terms, and the peak is antisymmetric with respect to κ, due to prefactor $(\kappa D)^{-1}$. The sign of its contribution to the diffuse scattering cross section is determined by the factor S_c. Thus, smoothly varying correlations between interfaces give rise to qualitatively the same shape of Bragg-diffraction peaks as completely correlated roughness of interfaces. However, the peaks due to completely uncorrelated roughness are governed by another factor, S_u, and follow the intensity of X-ray standing wave at interfaces. One can expect a qualitative transition from one extreme to the other in case of a fast decrease in correlations with distance between interfaces, when the assumptions made at the beginning of this section are not valid. This conclusion is confirmed by numerical calculations below.

5. Numerical calculations of diffuse scattering

5.1. Basic formulae

Although the approximate equations derived in the previous section are helpful for a qualitative analysis of diffuse scattering, they are not accurate enough to calculate the whole picture of diffuse scattering. In particular, they are not applicable when the incident or scattered wave is close to the region of total specular reflection. For an accurate evaluation of diffuse scattering on the basis of the reciprocity theorem (2), one has to calculate the undisturbed wave fields E^{in} and E^{out} in each layer. They can be represented as a sum of the transmitted (t) and reflected (r) waves:

$$E^{s(j)} = \sum_{m=\text{t,r}} E_m^{s(j)} \exp(\mathrm{i}\boldsymbol{K}_m^{s(j)}\boldsymbol{r}), \quad (21)$$

where $s = (\text{in, out})$. The amplitudes $E_t^{s(j)}$ and $E_r^{s(j)}$ and the wave vectors $\boldsymbol{K}_t^{s(j)}$ and $\boldsymbol{K}_r^{s(j)}$ in jth layer can be found by solving the boundary problem on each interface [31, 32]. Diffuse scattering is caused by non-ideal interfaces between layers. Substituting wave fields (21) for Eq. (2), one finds the contribution f_j to the amplitude of diffuse scattering due to jth interface as a sum of four terms

$$f_j = \frac{k^2}{4\pi}\sum_{m=\text{t,r}}\sum_{n=\text{t,r}} E_m^{\text{out}(j)}\delta\chi_j'(\boldsymbol{K}_m^{\text{out}(j)} + \boldsymbol{K}_n^{\text{in}(j)})E_n^{\text{in}(j)}. \quad (22)$$

In deriving Eq. (22), the wave field of jth layer was applied to both parts of the interface between layers j and $(j+1)$. This assumption can be crucial whenever we are close to the total reflection region where the wave fields differ essentially above and below the surface [25] but seems appropriate for larger angles of incidence and exit, where the wave fields vary only slightly at each interface and the diffracted wave is formed due to scattering at a sufficiently large number of interfaces. The differential cross section

$d\sigma/d\Omega = \langle |\sum_j f_j|^2 \rangle$ contains the sum of as large as 16 terms for each pair of the interfaces involving correlations $\langle \delta\chi_j'(\boldsymbol{Q}_1)\,\delta\chi_k'^*(\boldsymbol{Q}_2)\rangle$ between polarizability fluctuations on different interfaces [4, 18, 21]. Here $\boldsymbol{Q}_1$ and $\boldsymbol{Q}_2$ are two wave vectors from the set involved in Eq. (22).

A rough interface can be treated as a boundary between two media with the polarizabilities $\chi_{\rm id}^{(j)}$ and $\chi_{\rm id}^{(j+1)}$ randomly displaced by $u_j(\boldsymbol{\rho})$ from the mean position z_j of the interface. Here $\boldsymbol{\rho} = (x, y)$ is a coordinate vector in the plane of interface. Calculation of the correlation function is tedious but straightforward and we point out to the main steps only [4, 18, 21]. First, one has

$$\begin{aligned}\delta\chi_j'(\boldsymbol{Q}) &= \Delta\chi_j \int d^2\rho \int_{z_j}^{z_j+u_j(\boldsymbol{\rho})} dz \exp(-i\boldsymbol{Q}^j\boldsymbol{r}) \\ &= -\frac{i\Delta\chi_j}{Q_z^j}\exp(-iQ_z^j z_j) \\ &\quad\times \int d^2\rho\, \exp(-i\boldsymbol{q}_\perp\boldsymbol{\rho})\{\exp[-iq_z u_j(\boldsymbol{\rho})] - 1\},\end{aligned} \tag{23}$$

where $\Delta\chi_j = \chi_{\rm id}^{(j)} - \chi_{\rm id}^{(j+1)}$. Further calculation of correlation function $\langle \delta\chi_j'(\boldsymbol{Q}_1)\delta\chi_k'^*(\boldsymbol{Q}_2)\rangle$ involves the means $\langle \exp[i(Q_{1z}^j u_j - Q_{2z}^{k*} u_k)]\rangle$ which are calculated for Gaussian random variables u_j with the aid of general formula [33] $\langle \exp(\sum_j \alpha_j x_j)\rangle = \exp(\frac{1}{2}\sum_{jk}\alpha_j\alpha_k\langle x_j x_k\rangle)$, where α_j are constants and x_j are Gaussian random variables. Finally, the correlation function can be represented in the form of Eq. (6), where

$$\begin{aligned}C_{jk}(Q_{1z}, Q_{2z}, \boldsymbol{q}_\perp) &= \frac{S}{Q_{1z}^j Q_{2z}^{k*}}\exp[-(Q_{1z}^{j\,2}\sigma_j^2 + Q_{2z}^{k*\,2}\sigma_k^2)/2] \\ &\quad\times \int d^2\rho\, \exp(-i\boldsymbol{q}_\perp\boldsymbol{\rho})\{\exp[Q_{1z}^j Q_{2z}^{k*}\mathscr{K}_{jk}(\boldsymbol{\rho})] - 1\},\end{aligned} \tag{24}$$

S is the scattering area, $\sigma_j^2 = \langle [u_j(\boldsymbol{\rho})]^2\rangle$ and $\mathscr{K}_{jk}(\boldsymbol{\rho}) = \langle u_j(0)u_k(\boldsymbol{\rho})\rangle$. We note here that the term $\exp[i(Q_{1z}^j z_j - Q_{2z}^k z_k)]$ of Eq. (6), which causes diffuse intensity to concentrate on the sheets in case of correlated roughness of periodic interfaces, was omitted in the corresponding equation of Ref. [4] and included implicitly in the amplitude terms.

In the case of small rms height of roughness σ_j or small wave vector transfers Q_z, so that $\sigma_j Q_z \ll 1$, Eq. (24) is simplified to $C_{jk}(\boldsymbol{q}_\perp) = \mathscr{K}_{jk}(\boldsymbol{q}_\perp)$, where $\mathscr{K}_{jk}(\boldsymbol{q}_\perp)$ is the Fourier transform of $\mathscr{K}_{jk}(\boldsymbol{\rho})$.

5.2. Correlation functions

Now, we have to define an explicit form for the correlation function $\mathscr{K}_{jk}(\boldsymbol{q}_\perp)$ in Eq. (24). For $j = k$ the correlation functions are commonly taken, after Ref. [25], as

$$\mathscr{K}_{jj}(\boldsymbol{\rho}) = \langle u_j(0)u_j(\boldsymbol{\rho})\rangle = \sigma_j^2\exp[-(\rho/\xi_j)^{2h}], \tag{25}$$

where σ_j and ξ_j are the rms height and the lateral correlation length of roughness at jth interface, and $3 - h$ is a fractal dimension ($0.5 \leqslant h \leqslant 1$).

For $j \neq k$ there is a variety of suggestions, which can be divided into models assuming non-accumulated [2, 10, 34] and accumulated [4, 11] roughness. In the first case, the correlations between interfaces are assumed to depend on the distance between them. For example, in the model by Ming et al. [2] the correlation function has the form

$$\mathscr{K}_{jk}(\boldsymbol{\rho}) = \sqrt{\mathscr{K}_{jj}(\boldsymbol{\rho})\mathscr{K}_{kk}(\boldsymbol{\rho})}\exp(-|z_j - z_k|/\xi_{\rm vert}), \tag{26}$$

where $\xi_{\rm vert}$ is a vertical correlation length of roughness. Usually, one takes $\mathscr{K}_{nn}$ equal to each other, $\mathscr{K}_{nn} = \mathscr{K}$. The correlations of interfacial roughness can vary between two limits considered in Section 4, uncorrelated interface roughness, $\mathscr{K}_{jk}(\boldsymbol{\rho}) = \mathscr{K}(\boldsymbol{\rho})\delta_{jk}$, at $\xi_{\rm vert} \to 0$, and completely correlated (replicated) roughness, $\mathscr{K}_{jk}(\boldsymbol{\rho}) = \mathscr{K}(\boldsymbol{\rho})$, at $\xi_{\rm vert} \to \infty$.

Spiller et al. [11] suggested considering that the interfaces are formed successively one after another, starting with the substrate and with the layers repeating long-wavelength modulations in the interface positions, whereas the short-wavelength roughness of an interface is smeared out and appears on the next interface independently. A spatial frequency dependence of the number of interfaces involved in correlations has been observed recently [10, 12]. This assumption leads to the accumulation of roughness and brings the following recurrent formula for the Fourier transforms of displacements of subsequent interfaces [11]: $u_j(\boldsymbol{f}) = h_j(\boldsymbol{f}) + a_j(\boldsymbol{f})u_{j+1}(\boldsymbol{f})$, where $\boldsymbol{f}$ is a two-dimensional wave vector in the interface plane, h_j are uncorrelated random displacements acquired at jth interface ($\langle h_j h_k\rangle = 0$ for $j \neq k$). The function a_j governs the roughness transfer; it was taken in Ref. [11] on the assumption of diffusion-like roughness propagation $a_j(\boldsymbol{f}) = \exp[-v_j(z_{j+1} - z_j)f^2]$, where v_j are relaxation parameters and $z_{j+1} - z_j > 0$ is the thickness of jth layer ($z = 0$ is the multilayer surface and $z = z_N$ is the substrate–multilayer interface).

Here we derive the correlation function of displacements $\mathscr{K}_{jk}(\boldsymbol{\rho})$ for this model on the assumption that the relaxation parameters are equal to each other, $v_j = v$. Starting from the substrate roughness $u_N \equiv h_N$ and iteratively expressing u_j's, we arrive at

$$\begin{aligned}\mathscr{K}_{jk}(\boldsymbol{\rho}) &= \sum_{n=\max(j,k)}^{N}\int d^2 f\, \langle h_n^2(\boldsymbol{f})\rangle \\ &\quad\times \exp[-v(2z_n - z_j - z_k)f^2]\exp(i\boldsymbol{f}\boldsymbol{\rho}),\end{aligned} \tag{27}$$

where $\langle h_n^2(\boldsymbol{f})\rangle$ can be expressed in terms of the correlation functions $\mathscr{K}_n(\boldsymbol{\rho})$ describing the acquired interface

roughness

$$\langle h_n^2(\boldsymbol{f})\rangle = (2\pi)^{-2}\int \mathrm{d}^2\rho\,\langle h_n(0)h_n(\boldsymbol{\rho})\rangle \exp(\mathrm{i}\boldsymbol{f}\boldsymbol{\rho}) \equiv \int \mathrm{d}^2\rho\,\mathscr{K}_n(\boldsymbol{\rho})\exp(\mathrm{i}\boldsymbol{f}\boldsymbol{\rho}). \tag{28}$$

As it follows from Eq. (27), the correlation between two interfaces, jth and kth, is completely determined by roughness acquired on the way from substrate to that interface of two which is closer to the substrate and does not depend on the way between these two interfaces.

Denoting $p_n^2 = 4v(2z_n - z_j - z_k)$ and making the Fourier transform in Eq. (27) after the substitution of Eq. (28), we obtain

$$\mathscr{K}_{jk}(\boldsymbol{\rho}) = \sum_{n=\max(j,k)}^{N} \frac{1}{\pi p_n^2}\int \mathrm{d}^2\rho'\,\mathscr{K}_n(\rho')\exp[-(\rho'+\boldsymbol{\rho})^2/p_n^2]. \tag{29}$$

The limit $v \to 0$, implying complete roughness transfer at all spatial frequencies and the assumption of similar acquired roughness at all interfaces ($\mathscr{K}_n(\boldsymbol{\rho}) = \mathscr{K}(\boldsymbol{\rho})$ at $n < N$), gives rise to the correlation function [4] $\mathscr{K}_{jk}(\boldsymbol{\rho}) = \mathscr{K}_N(\boldsymbol{\rho}) + [N - \max(j,k)]\mathscr{K}(\boldsymbol{\rho})$, where $\mathscr{K}_N(\boldsymbol{\rho})$ is the correlation function of the substrate surface.

Let us consider the more general case $v \neq 0$. The correlation functions $\mathscr{K}_n(\boldsymbol{\rho})$ can be assumed in the form (25). As noted in Ref. [3], the major part of the diffuse scattering pattern has a weak dependence on the fractal dimensionality h in this function. (The exceptions are only the regions close to the specular reflection strip in the reciprocal space.) Taking $h = 1$ (Gaussian distribution) and substituting correlation function (25) into Eq. (29) we obtain

$$\mathscr{K}_{jk}(\boldsymbol{\rho}) = \sum_{n=\max(j,k)}^{N} \sigma_n^2 \frac{\xi_n^2}{\xi_n^2 + p_n^2}\exp\left[-\frac{\boldsymbol{\rho}^2}{\xi_n^2 + p_n^2}\right]. \tag{30}$$

As clearly seen from Eq. (30), the lateral correlation length $\xi_n' = \sqrt{\xi_n^2 + p_n^2}$ of transferred roughness increases with increasing the separation between interfaces, whereas the effective rms of transferred roughness $\sigma_n' = \sigma_n/\sqrt{1 + p_n^2/\xi_n^2}$ decreases. In the limit $v \to \infty$ one has $\mathscr{K}_{j\neq k}(\boldsymbol{\rho}) = 0$, i.e., the absence of vertical correlations. In the opposite limit $v \to 0$ the roughness is completely transferred and accumulated, $\mathscr{K}_{jk}(\boldsymbol{\rho}) = \sum_{n=\max(j,k)}^{N} \sigma_n^2 \exp(-\boldsymbol{\rho}^2/\xi_n^2)$. In case where all ξ_n are equal to each other, $\xi_n = \xi$, we can introduce the vertical correlation length $\xi_{\mathrm{vert}} = \xi^2/v$. That is convenient for comparing this model with the model of non-accumulated roughness (26).

Now, we turn to the evaluation of the integral in Eq. (24). In most experiments, the integration over q_y (in the direction normal to the plane of specular reflection) is performed, due to a wide window of the X-ray detector. Then, Eq. (24) involves the integration over x only:

$$C_{jk}(Q_{1z}, Q_{2z}, q_x) = \frac{2S}{Q_{1z}^j Q_{2z}^{k*}}\exp[-(Q_{1z}^{j\,2}\sigma_j^2 + Q_{2z}^{k*\,2}\sigma_k^2)/2] \times \int_0^\infty \mathrm{d}x\cos(q_x x) \times\{\exp[Q_{1z}^j Q_{2z}^{k*}\mathscr{K}_{jk}(x)] - 1\}. \tag{31}$$

In general, the above integral has to be taken numerically. However, for the correlation function (26) the calculations can be greatly simplified, as suggested by Sinha [21]: the exponent in Eq. (31) can be expanded into power series taken up to ten terms. Then the calculations are reduced to the evaluation of integrals $\Gamma(p) = \int_0^\infty \mathrm{d}x\exp(-x^{2h})\cos(px)$, which can be tabulated in advance. For $h = 1$ as well as for $h = 0.5$ these integrals are taken analytically.

For the correlation function (30) the expansion is basically not helpful. Direct numerical integration is also difficult because the integrated function oscillates and generally contains many exponentials with different decay rates. However, at large $x \gg x_{\max} \simeq \max[\xi_n\sqrt{\ln(100|Q_{1z}^j Q_{2z}^{k*}|\sigma_n)}]$ the exponent in Eq. (31) can be expanded to the term linear over $\mathscr{K}_{jk}(x)$ and the corresponding integral can be evaluated analytically. Therefore, the range of numerical integration in Eq. (31) can be essentially diminished with the help of the following transformation:

$$\frac{2}{Q_{jk}}\int_0^\infty \mathrm{d}x\,[\exp(Q_{jk}\mathscr{K}_{jk}(x)) - 1]\cos(q_x x) = \mathscr{K}_{jk}(q_x) + 2\int_0^{x_{\max}} \mathrm{d}x\,\{Q_{jk}^{-1}[\exp(Q_{jk}\mathscr{K}_{jk}(x)) - 1] - \mathscr{K}_{jk}(x)\}\cos(q_x x), \tag{32}$$

where we denoted $\mathscr{K}_{jk}(x) = \sum_{n=\max(j,k)}^{N} \sigma_n'^{\,2}\exp(-x^2/\xi_n'^{\,2})$, and $Q_{jk} = Q_{1z}^j Q_{2z}^{k*}$, and

$$\mathscr{K}_{jk}(q_x) = 2\int_0^\infty \mathrm{d}x\,\mathscr{K}_{jk}(x)\cos(q_x x) = \sqrt{\pi}\sum_{n=\max(j,k)}^{N} \sigma_n'^{\,2}\exp(-\xi_n'^{\,2}q_x^2/4). \tag{33}$$

For weak correlations, when $|Q_{jk}|\sum_{n=\max(j,k)}^{N}\sigma_n'^{\,2} \ll 1$, the right-hand side of Eq. (33) is reduced to $\mathscr{K}_{jk}(q_x)$ and the numerical integration is not necessary at all. In particular, that can often take place for $j \neq k$.

5.3. Numerical examples

Let us compare the effect of change in vertical correlations of roughness for two models, non-accumulated and accumulated interface roughness. We start with the model

by Ming et al. (26) since it can be directly related to the analytical estimations of Section 4.

Fig. 2 presents the distributions of diffuse scattering intensity for different values of ξ_{vert} in Eq. (26). The computations have been performed for GaAs/AlAs superlattice consisting of 20 periods of 95 Å GaAs and 125 Å AlAs on a GaAs substrate, and the X-ray wavelength $\lambda = 1.5$ Å. The parameters of interfacial roughness $\sigma = 8.6$ Å, $h = 1$, and $\xi = 2000$ Å have been chosen the same as in Ref. [4]. The data have been integrated over q_y. The left column shows the iso-intensity maps. The intensity of diffuse scattering is calculated in the region available in X-ray specular reflection experiments, the wave vector transfer being restricted by positive values of the angles of incidence and exit. The right column shows the sections of diffuse intensity distributions along $q_x = 0$ (along the specular reflection strip).

The most pronounced feature due to the correlations of roughness of interfaces is the concentration of the intensity on equidistantly spaced RDS sheets which are perpendicular to q_z-axis at small q_x and bent with increasing q_x [1, 2, 4, 6–10, 12, 21]. Their formation with increasing ξ_{vert} is clearly seen in Fig. 2 and is well understood in the limiting case of completely correlated roughness, Eqs. (8) and (9). The RDS maxima are the lines $Q_z = 2\pi m/D$, the curvature of the sheets is due to the refraction of X-rays in the slab possessing the mean polarizability $\chi_0 = (\chi_1 d_1 + \chi_2 d_2)/D$. In addition, the diffuse scattering at all ξ_{vert} possesses the singularities along the lines where either the incident or the scattered wave occurs in the Bragg-diffraction condition. These lines form a regular mesh on the iso-intensity maps in Fig. 2.

The intensity distributions along sections $q_z = \text{const}$ (corresponding to ω-scans in experiment) are presented in Fig. 3. Lines 1 and 3 in Fig. 3 correspond to uncorrelated roughness and lines 2 and 4 to completely correlated one. All the lines exhibit the Bragg-diffraction peaks when crossing the mesh of Fig. 2. For the case of uncorrelated roughness, each peak is completely characterized by the order m of the diffraction vector $H = 2\pi m/D$ and consists of maximum and minimum, whose sequence is controlled by the factor S_u, Eq. (14). The peak profile does not depend on q_z for a given diffraction order m, as follows from Eq. (13) and can be seen following the Bragg diffraction lines (regular mesh in Fig. 2), indicated schematically by dotted lines in Fig. 3. The intensity of the peak smoothly decreases with increasing m due to the variation of correlation function C. For the value $d_1/D =$

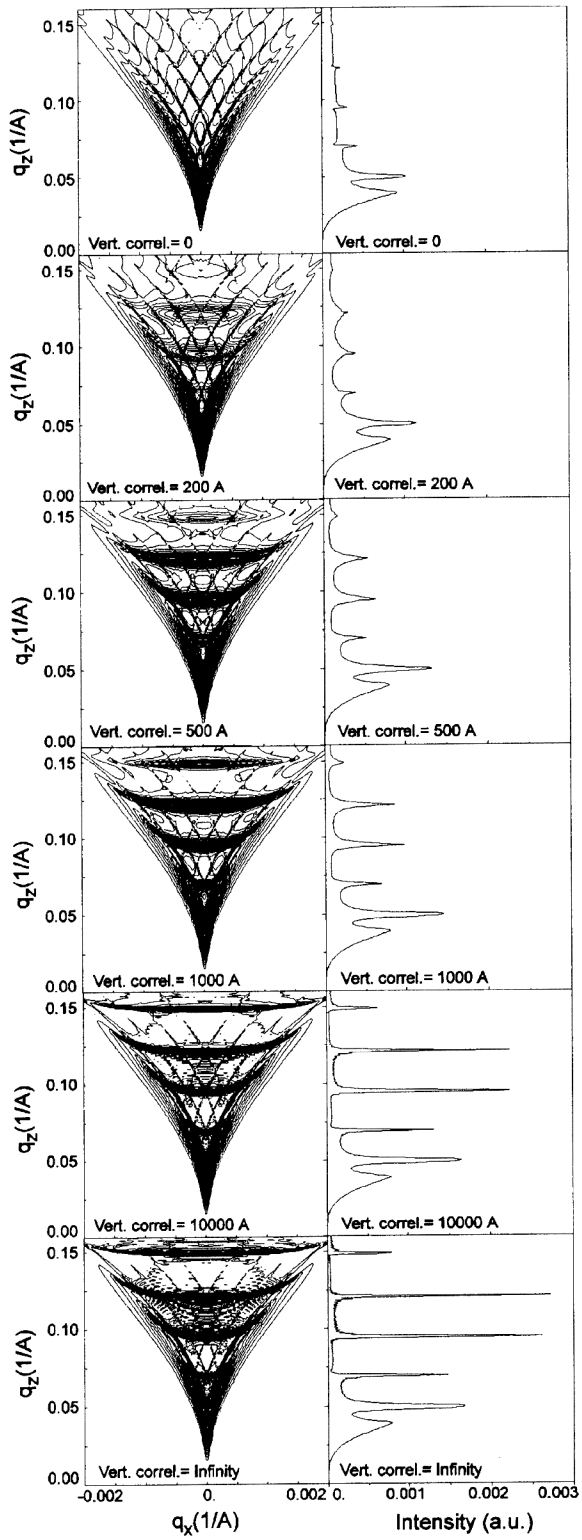

Fig. 2. Formation of resonant sheets in X-ray diffuse scattering from periodic multilayers with an increase in the vertical correlation length of interface roughness. The left column presents iso-intensity maps and the right one shows the sections of diffuse intensity at $q_x = 0$. The rhomb-like mesh in the maps is due to the Bragg conditions for either incident or scattered X-ray waves. For the parameters of computations, see text.

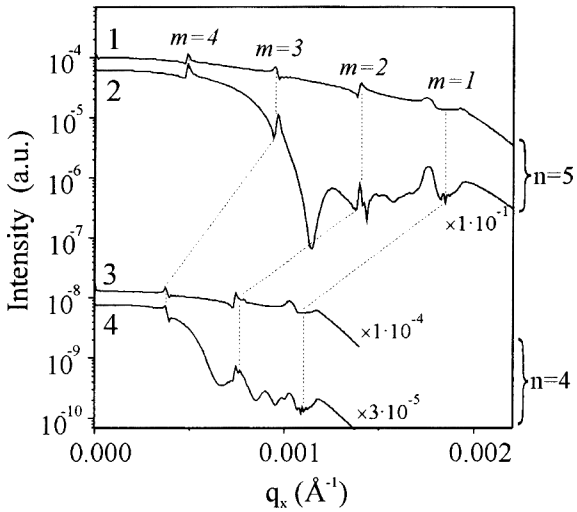

Fig. 3. Sections of diffuse intensity along q_x at constant q_z for interface roughness possessing no correlations at different interfaces (lines 1 and 3) and complete vertical correlation through multilayer stack (lines 2 and 4). Lines 1 and 2 correspond to the section along the 5th resonance sheet ($q_z = 0.1487$ Å^{-1}) and lines 3 and 4 to that along the 4th sheet ($q_z = 0.1212$ Å^{-1}).

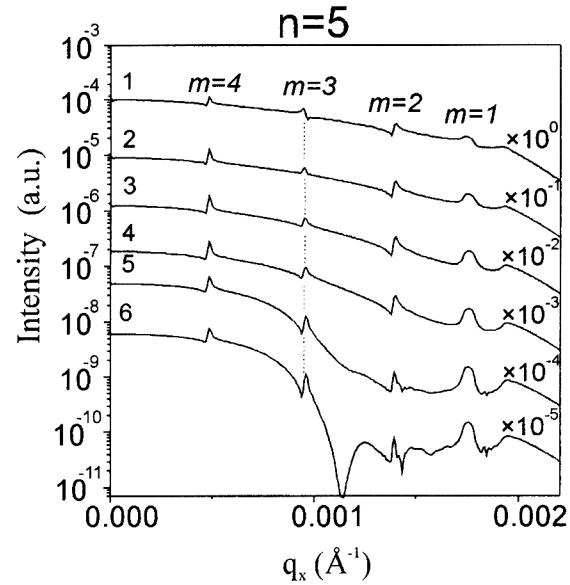

Fig. 4. Transformation of Bragg peaks in the section along the 5th resonance sheet with an increase in the vertical correlation length of interface roughness. Lines 1 to 6 correspond to $\xi_{\text{vert}} =$ 0, 200, 500, 1000, 10 000, ∞ Å, respectively. The vertical dotted line marks transformation of the 3rd Bragg peak.

0.43 used in the calculations and for $m = 2, 3$, and 4, Eq. (14) gives $S_u = -0.77$, 0.97, and -0.98, respectively. Thus, S_u changes its sign for $m = 2$, 3, 4 in the order $(-, +, -)$ and in the same order changes the sense of the features of the Bragg peaks: the 3rd order peak on curves 1 and 3 of Fig. 3 has the opposite sense with respect to the 2nd and 4th peaks.

For the case of correlated roughness, the sense of the peaks is controlled by another factor, S_c, Eq. (19), and depends on the order n of RDS sheet ($Q_z = 2\pi n/D$). For $n = 5$ and $m = 2, 3$, and 4, one has $S_c = -0.34$, -0.15, and -0.15, i.e. $(-, -, -)$. Accordingly, the three peaks on the curve 2 of Fig. 3 have the same sense and, in particular, the 3rd order peak possesses *opposite contrasts* in cases of correlated and uncorrelated roughness. For $n = 4$ (curve 4 of Fig. 3) one has $S_c = -0.14$ and 0.59 for $m = 2$ and 3, respectively, and the sense of the 3rd peak is preserved (cf. curves 2 and 4 in Fig. 3). Thus, the effect of the two limits of completely correlated and uncorrelated roughness on qualitative features of the Bragg peaks becomes obvious in Fig. 3 particularly for the 3rd order peak, which possesses opposite contrasts for the two cases at $n = 5$ and equal contrasts at $n = 4$.

Fig. 4 illustrates the process of transforming the 3rd peak at $n = 5$ with increasing vertical correlation. One can see that the peak contrast becomes already inverted at minor vertical correlations, the parameter $\xi_{\text{vert}} = 200$ Å being less than one multilayer period, thus confirming predictions of Section 4.4.

The Bragg singularity at $m = 1$ in Fig. 3 must be discussed separately because it is formed by the dynamical diffraction of the incident wave. The width of the peak is Λ_1^{-1}, the inverse value of the extinction length for this reflection. Since the extinction length is smaller than the multilayer thickness L, the peak width exceeds that of the kinematical peaks ($m = 2$, 3, 4), which are proportional to L^{-1}. The decrease in penetration depth in the total reflection region gives rise to a broad minimum with the peaks at the edges of that region where the penetration depth essentially increases. This behavior is similar to that in the standing wave problem if the depth of secondary radiation yield exceeds the extinction length [35].

Fig. 5 illustrates the same process as in Fig. 4 for the accumulated roughness model, i.e. for the correlation function (30). The parameters of calculations are the same as in previous figures with the exception of rms roughness: $\sigma_{n<N} =$ 1.6 Å and $\sigma_N = 8.6$ Å. The rms roughness heights at interfaces depend on the vertical correlation length: for example, the value of σ_1 at the top interface (the surface) varies from 1.6 Å at $\xi_{\text{vert}} = 0$ to 13.3 Å at $\xi_{\text{vert}} = \infty$.

By comparing Figs. 4 and 5, one can see that, with increasing the vertical correlation length, the diffuse intensity in Spiller's model increases first for small q_x, due to prior transferring of the long-wavelength interface roughness. It can also be noted that the contrast of the 3rd Bragg peak inverts later than in the non-accumulated roughness model, though this peak changes its sense at a rather small vertical

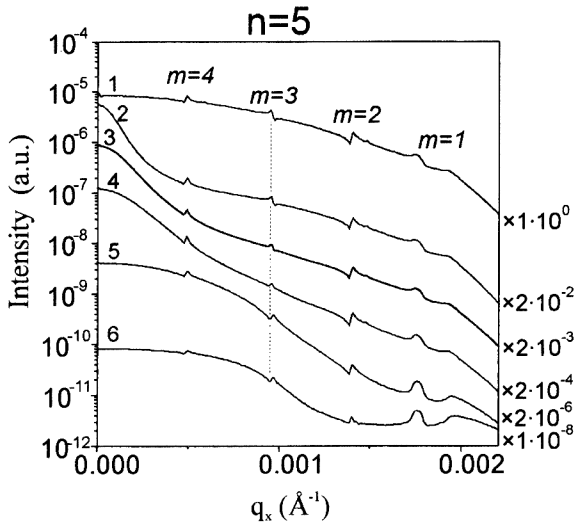

Fig. 5. The same as in Fig. 4 for the accumulated surface roughness model.

correlation length as well (ξ_{vert} is less than 5 periods). In this model the inversion of the contrast occurs at smaller ξ_{vert} for peaks located closer to $q_x = 0$ and in the case of small lateral correlation length ξ of roughness (the sensitivity of peak contrast to vertical correlations is increased at $q_x|_{\text{peak}} \ll 1/\xi$).

6. Conclusions

We have analyzed the Bragg-diffraction peaks in X-ray diffuse scattering due to interface roughness from periodic multilayers. The factors controlling the contrast of these singularities have been found analytically and confirmed by numerical calculations. For completely uncorrelated roughness of interfaces, Bragg singularities follow the intensity of the X-ray standing wave at the interfaces. It has been proven that the contrast of these peaks can invert due to minor correlations between roughness which are insufficient for formation of the resonance diffuse scattering sheets. This sensitivity is especially pronounced in the case of non-accumulated interface roughness. The inversion of the Bragg peak sense might be helpful in studies of minor correlations between rough interfaces.

Acknowledgements

One of us (V.K.) is indebted to S.K. Sinha and V. Holý for stimulating discussions.

References

[1] Y.H. Phang et al., Appl. Phys. Lett. 60 (1992) 2986.
[2] Z.H. Ming et al., Phys. Rev. B 47 (1993) 16373.
[3] V. Holý et al., Phys. Rev. B 47 (1993) 15896.
[4] V. Holý and T. Baumbach, Phys. Rev. B 49 (1994) 10669.
[5] S.K. Sinha et al., Physica B 198 (1994) 72.
[6] J.B. Kortright, J. Appl. Phys. 70 (1991) 3620.
[7] D.E. Savage et al., J. Appl. Phys. 69 (1991) 1411.
[8] X. Jiang, T.H. Metzger and J. Peisl, Appl. Phys. Lett. 61 (1992) 904.
[9] D.G. Stearns, J. Appl. Phys. 71 (1992) 4286.
[10] Y.H. Phang, D.E. Savage, R. Kariotis and M.G. Lagally, J. Appl. Phys. 74 (1993) 3181.
[11] E. Spiller, D. Stearns and M. Krumrey, J. Appl. Phys. 74 (1993) 107.
[12] T. Salditt, T.H. Metzger and J. Peisl, Phys. Rev. Lett. 73 (1994) 2228.
[13] R. Chiarello, V. Panella, J. Krim and C. Thompson, Phys. Rev. Lett. 67 (1991) 3408.
[14] C. Thompson et al., Phys. Rev. B 49 (1994) 4902.
[15] P.P. Swaddling et al., Phys. Rev. Lett. 73 (1994) 2232.
[16] D.K. Schwartz et al., Phys. Rev. A 41 (1990) 5687.
[17] M.K. Sanyal, S.K. Sinha, K.G. Huang and B.M. Ocko, Phys. Rev. Lett. 66 (1991) 628.
[18] J. Daillant and O. Bélorgey, J. Chem. Phys. 97 (1992) 5824.
[19] J. Daillant and O. Bélorgey, J. Chem. Phys. 97 (1992) 5837.
[20] A. Gibaud, N. Cowlam, G. Vignaud and T. Richardson, Phys. Rev. Lett. 74 (1995) 3205.
[21] S.K. Sinha, J. Phys. III France 4 (1994) 1543.
[22] A.V. Andreev, A.G. Michette and A. Renwick, J. Modern Opt. 35 (1988) 1667.
[23] S.K. Sinha, in: Neutron Scattering in Materials Science, eds. D.A. Neumann et al. (Materials Research Society, Boston, MA, 1995) Vol. 376.
[24] D.K.G. de Boer, A.J.G. Leenaers and R.M. Wolf, J. Phys. D 28 (1995) A227.
[25] S.K. Sinha, E.B. Sirota, S. Garoff and H.B. Stanley, Phys. Rev. B 38 (1988) 2297.
[26] M. von Laue, Ann. Phys. 23 (1935) 705.
[27] V.E. Dmitrienko and V.M. Kaganer, Metallofizika 9 (1987) 71 [English transl.: Phys. Metals 9 (1990) 102].
[28] L.D. Landau and E.M. Lifshitz, Electrodynamics of Continuous Media (Pergamon Press, London, 1960).
[29] R.W. James, The Optical Principles of the Diffraction of X-Rays (Bell, London, 1950).
[30] L.D. Landau and E.M. Lifshitz, Quantum Mechanics (Pergamon Press, Oxford, 1981).
[31] F. Abeles, Ann. Phys. (Paris) 3 (1948) 504; 5 (1950) 596.
[32] L.G. Parratt, Phys. Rev. 95 (1954) 359.
[33] L.D. Landau and E.M. Lifshitz, Statistical Physics, Part 1 (Pergamon Press, Oxford, 1980).
[34] J.-P. Schlomka et al., Phys. Rev. B 51 (1995) 2311.
[35] B.W. Batterman, Phys. Rev. 133 (1964) 759.